values can be obtained when radical dimerization rates are known from flash photolysis studies.[31]

Acknowledgment. We thank the Natural Sciences and Engineering Research Council, Ottawa, for support and Professor T. L. Brown for communicating his results to us prior to publication.

Appendix

Derivation of the Rate Equations. If $\cdot Mn(CO)_4(PPh_3)$ is represented by A we have, for the reactions shown in Scheme I

$$R = -d[A_2]/dt = (k_5 + k_9)[A_2] - k_{-5}[A]^2 - k_{-9}[A_2^*] = 0.5k_{12}[A(RX)] + k_{14}[A(CO)]$$

Since the radicals enclosed in the rectangle in Scheme I are considered to be in labile equilibrium with each other[40] we have

$$[A] = [A(RX)]/K_{11}[RX] = [A(CO)]/K_{13}[CO]$$

and

$$[A(CO)] = K_{13}[CO][A(RX)]/K_{11}[RX]$$

whence

$$R = [A(RX)]\{0.5K_{11}k_{12}[RX] + K_{13}k_{14}[CO]\}/K_{11}\,[RX] = a[A(RX)]$$

and

$$[A]^2 = [A(RX)]^2/K_{11}^2[RX]^2 = R^2/a^2K_{11}^2[RX]^2$$

Similarly, $[A][A(RX)] = R^2/a^2K_{11}[RX]$ and

$$d[A_2^*]/dt = k_9[A_2] - \{k_{-9} + k_{10}[RX]\}[A_2^*] + k_{-10}[A][A(RX)] = 0$$

i.e.

$$[A_2^*] = \{k_9[A_2] + k_{-10}R^2/a^2K_{11}[RX]\}/\{k_{-9} + k_{10}[RX]\}$$

whence

$$R = k_5[A_2] + k_9[A_2]\{1 - k_{-9}/(k_{-9} + k_{10}[RX])\} - \{k_{-9}k_{-10}R^2/(k_{-9} + k_{10}[RX])a^2K_{11}[RX]\} - k_{-5}R^2/a^2k_{11}^2[RX]^2$$

Taking $k_{obsd} = R/[A_2] = R/C$ we have

$$k_{obsd} = k_5 + k_9k_{10}[RX]/(k_{-9} + k_{10}[RX]) - \{k_{-9}k_{-10}/(k_{-9} + k_{10}[RX]) + k_{-5}/K_{11}[RX]\}k_{obsd}^2C/a^2K_{11}[RX]$$

When $k_{10}[RX] \gg k_{-9}$

$$k_{obsd} = k_5 + k_9 - (k_{-9}k_{-10}/k_{10} + k_{-5}/K_{11})k_{obsd}^2C/a^2K_{11}[RX]^2$$

which is identical with eq 18 when a is expressed in full.

An equation for substitution reactions in the absence of CO can be derived in exactly the same way. The reactions involving CO in Scheme I are ignored, and RX in reactions 10 and 11 is replaced by L. Reaction 12 then involves formation of $\cdot Mn(CO)_4L$ from $\cdot Mn(CO)_4(PPh_3)(L)$ and is immediately followed by reaction with $\cdot Mn(CO)_4(PPh_3)$ to form $Mn_2(CO)_8(PPh_3)(L)$. Thus, each time reaction 12 occurs two radicals are lost from the steady-state assemblage and $R = k_{12}[\cdot Mn(CO)_4(PPh_3)(L)]$, i.e., the statistical factor of 0.5 no longer appears as it did for reactions with RX. The rate equation obtained for substitution by combined spontaneous and induced homolysis is then easily shown to be

$$k_{obsd} = k_5 + k_9 - (k_{-5} + k_{-9}k_{-10}K_{11}/k_{10})k_{obsd}^2C/k_{12}^2K_{11}^2[L]^2$$

provided $k_{10}[L] \gg k_{-9}$, as before.

(40) Rate equations so derived fit very well with the data, and we have not been able to derive rate equations without making this simplifying assumption.

Registry No. $Mn_2(CO)_8(PPh_3)_2$, 10170-70-4; CO, 630-08-0; $P(OPh)_3$, 101-02-0; O_2, 7782-44-7; $C_{16}H_{33}I$, 544-77-4; $C_2H_2Cl_4$, 25322-20-7; P-*n*-Bu_3, 998-40-2; $P(OEt)_3$, 122-52-1; NO, 10102-43-9; $Mn_2(CO)_{10}$, 10170-69-1.

Supplementary Material Available: Tables of rate constants (4 pages). Ordering information is given on any current masthead page.

Fundamental Study of the Oxidation of Butane over Vanadyl Pyrophosphate

Marc A. Pepera, James L. Callahan, Michael J. Desmond,* Ernest C. Milberger, Patricia R. Blum, and Noel J. Bremer

Contribution from the Corporate Research Department of The Standard Oil Company, Cleveland, Ohio 44128. *Received December 14, 1984*

Abstract: The oxidation of butane as catalyzed by β-$(VO)_2P_2O_7$ was studied as a function of the separate catalyst oxidation and reduction steps. The vanadyl pyrophosphate was found to have a reversible oxidation capacity approaching one oxygen molecule per two surface vanadium centers. The reduction reaction of the catalyst surface was found to be first order in butane and the oxidation reaction was found to be first order in oxygen. These two reactions occur in distinct, separate steps, a behavior similar to that exhibited by catalysts which can utilize lattice oxygen from the bulk in oxidation reactions. Pulse studies over the catalyst, involving the use of ^2H- and ^{18}O-labeled compounds, revealed a very dynamic surface for β-$(VO)_2P_2O_7$ at 400 °C. All oxygen and hydrogen atoms in the surface layer were found to be in fast exchange relative to the time scale of the conversion of butane to maleic anhydride and combustion products. Experiments with deuterium-labeled butane revealed that the rate-controlling step for butane oxidation was the irreversible activation of a methylene carbon–hydrogen bond in butane on the catalyst surface. Vanadium(IV) sites on the catalyst surface are proposed to be responsible for both the chemisorption of oxygen and the activation of butane. The combination of a V(V) $\rightleftharpoons$ V(IV) couple and the dynamic nature of the surface layer are thought to be mechanistically important for the 14-electron oxidation of butane to maleic anhydride.

The petrochemical industry currently relies on unsaturated molecules obtained from the refining process to produce derivative chemicals. Recent efforts have been directed at the substitution of paraffinic molecules for the more valuable unsaturates in some of these processes. The challenge of activating a C–H bond at a saturated carbon center with the conversions and selectivities required for an industrial process is a monumental one. Over the last decade, processes which form maleic anhydride from the oxidation of butane have significantly displaced previous technology which relied on benzene. This conversion represents a very

0002-7863/85/1507-4883$01.50/0

successful substitution of paraffin for unsaturate.[1]

This paper reports a fundamental study of the reaction of butane over one of the catalytically important phases for the process, β-$(VO)_2P_2O_7$. Many compositions containing this phase have been successfully used as heterogeneous catalysts under conditions where the selectivites to maleic anhydride are in excess of 50% at high conversions.[2] The ability of this material to activate butane for selective oxidation is unusual, and the mechanisms are not yet well understood.

Many oxidation catalysts react with a hydrocarbon by utilizing bulk lattice oxygen, thereby becoming reduced in the process. The reduced metal oxide catalyst will then react with molecular oxygen to complete the effectively catalytic cycle. This redox mechanism of metal oxides was first described in the literature by Mars and van Krevelen.[3] The oxidation of butane to maleic anhydride is a 14-electron process which consumes 3.5 molecules of oxygen. The complete combustion of butane to CO_2 is a 26-electron process requiring 6.5 oxygen molecules. Therefore, it is of interest to know how much oxygen is available from β-$(VO)_2P_2O_7$ to perform the oxidation reaction relative to the participation of physisorbed or gas-phase molecular oxygen.

Previous investigations of the catalytic activity of VPO_x formulations have focused on the use of both butenes[4] and butane[5] as feedstocks. Studies were carried out in the continuous mode, most often in the presence of excess oxygen. The product distributions from the reactions of butenes contained various amounts of butadiene,[6] furan, and crotonaldehyde in addition to maleic anhydride, CO_2, and CO. A study[7] with 1-butene as a feedstock indicated very poor selectivity for maleic anhydride when using β-$(VO)_2P_2O_7$ in the absence of gas-phase oxygen. Simple oxydehydrogenation and allylic oxidation were the predominate reactions observed. A kinetic study[5a] using butane as a feedstock has indicated that the reaction proceeds between butane and oxygen in a manner consistent with the Mars–van Krevelen rate expression. A recent investigation[5c] reacted butane in the absence of oxygen over $(VO)PO_4$ phases and concluded that V(V)-related species were responsible for the activation of the butane in the direction of maleic anhydride formation.

In this study, the oxidation of butane and the reoxidation of β-$(VO)_2P_2O_7$ will be investigated as separate steps utilizing a pulse microreactor in order to gain further insight into the mechanism of the reaction and the role of the phase as a catalyst.

Experimental Section

β-$(VO)_2P_2O_7$ Preparation.[2b,8] Vanadium pentaoxide (909.5 g from Alfa) was stirred into 13 L of technical-grade isobutyl alcohol. Orthophosphoric acid (1196 g) dissolved in 2 L of isobutyl alcohol was then added to form a dark-yellow slurry which gradually darkened upon heating to reflux temperature (approximately 103–108 °C). After several hours, the mixture was cooled with continued stirring. A light-blue product was isolated by filtration and dried at room temperature under vacuum. The solid was washed with 1 L of isobutyl alcohol and dried under vacuum followed by 2.5 h at 145 °C. The blue product was analyzed to be $(VO)HPO_4 \cdot 0.5H_2O$ $[(VO)_2P_2O_7 \cdot 2H_2O]$[9] and exhibited the X-ray diffraction pattern listed in Table I.

The vanadyl hydrogen phosphate hemihydrate was then calcined at 400 °C in air to produce a green solid. An air/butane mixture was then passed over the phosphate at 400 °C until steady-state conversion of butane to maleic anhydride was well established. The reactor was then cooled, and the solid was recovered and shown to be β-$(VO)_2P_2O_7$ by elemental, redox titration, and X-ray (Table I) analyses.

Table I. X-ray Diffraction[a] Data for $(VO)HPO_4 \cdot 0.5H_2O$ and Reaction Equilibrated β-$(VO)_2P_2O_7$

$(VO)HPO_4 \cdot 0.5H_2O$		β-$(VO)_2P_2O_7$	
d, A	I/I_0 (×100)	d, A	I/I_0 (×100)
5.72	74	6.32	18
4.81	6	5.72	8
4.53	43	4.81	18
4.10	5	3.90	100
3.68	33	3.15	98
3.30	46	2.99	47
3.12	20	2.67	14
2.94	100	2.45	12
2.80	15	2.37	4
2.67	11		
2.61	7		
2.56	2		
2.46	2		
2.41	10		

[a] Cu Kα radiation, 5–40° scan.

Pulse Redox Studies. The pulse microreactor studies used 0.50 g of 10–30-mesh particles of vanadyl pyrophosphate in a stainless steel tubular reactor with an internal diameter of 1.11 cm. The resulting 0.57 cm high catalyst bed with a height-to-width ratio of 0.51 minimized the effects of concentration and temperature differences which occur from the top to bottom when reactions take place in a fixed bed configuration. Heating of the reactor tube was achieved by placing it in a temperature-controlled split block furnace. The experiments in this study were carried out with a catalyst temperature of 400 °C, with heating being controlled by monitoring the microreactor wall temperature at the midpoint of the catalyst bed.

The reactor assembly was interfaced between thermostated gas pulse/flow control and gas chromatography sections. A flow of helium gas was regulated by a Brooks Model 5850 mass flow controller, and O_2, butane, or air/butane pulses were introduced into the He stream from calibrated sample loops via a six-port Valco rotary valve. After traversing the reactor, the gas stream passed through a water-cooled condenser which served to remove non-volatile products such as maleic anhydride before the gas chromatography section.

The cooled pulse then entered a sample-transfer system thermostated at 125 °C, which contained a loop monitored by thermal conductivity detectors at the entrance and exit. When the pulse was contained in the loop, it was backflushed with a secondary helium stream (0.69 MPa) into the gas chromatography. The GC compartment was kept at 40 °C, and the 100 mL per minute flow was split to two parallel columns and then recombined before the thermal conductivity detector. The combination of 1.22 m by 0.32 cm stainless steel 45/60 molecular sieve 13X and a 7.32 m by 0.32 cm stainless steel 20% bis(2-methoxyethyl) adipate–80/100 Chromosorb P AW columns allowed for the detection and analysis of O_2, N_2, C_1–C_4 hydrocarbons, CO, and CO_2 in amounts in excess of approximately 1×10^{-8} mol.

Conversion and yields were calculated based on the amount of butane or oxygen pulsed over the catalyst. Routinely, the condensable products were not analyzed because of unacceptable analysis times for the pulse sequence experiments. The unaccounted butane was assumed to be converted to maleic anhydride. A number of control experiments which examined the combined condensable (−78 °C) product from a series of ten, single butane pulse redox cycles, as well as another set of experiments which examined the product from the reduction of the vanadyl pyrophosphate until constant butane breakthrough was observed, revealed the presence of only maleic anhydride in addition to unreacted butane via GC–mass spectrometry. The GC analyses routinely performed could detect gaseous products to a level of less than 0.1% of the pulse butane content.

Studies with Labeled Compounds. ^2H- and ^{18}O-labeled compounds were obtained from MSD Isotopes.

1. Deuterated Catalyst Studies. β-$(VO)_2P_2O_7$ (0.5 g) which had been equilibrated under oxygen was deuterated by passing 1.0 g of ^2H_2O (99.75 atom % ^2H) in flowing He over the reactor bed at 400 °C continuously over a period of a few minutes. The system was allowed to equilibrate until no steam was exiting the reactor. Following deuteration, n-butane or maleic anhydride was passed over the catalyst to determine the extent of H–D exchange.

2. Labeled Butane Studies. [2.2.3.3-$^2H_4$]-n-Butane and [1.1.1.4.4.4-$^2H_6$]-n-butane (98 atom % ^2H) were placed into reservoirs maintained

(1) Varma, R. A.; Saraf, D. N. *Ind. Eng. Chem. Prod. Res. Dev.* **1979**, *8*, 7.

(2) (a) Mount, R. A.; Rafelson, H. US Patent 3 330 354, 1975. (b) Schneider, R. A. US Patent 3 864 280, 1975. (c) Straus, A. E. US Patent 4 094 888, 1978.

(3) Mars, P.; van Krevelen, D. W. *Chem. Eng. Sci. (Spec. Suppl.)* **1954**, *3*, 41.

(4) (a) Ai, M. *Bull. Chem. Soc. Jpn.* **1970**, *43*, 3490. (b) Varma, R. L.; Saraf, D. N. *J. Catal.* **1978**, *55*, 361. (c) Centi, G.; Manenti, I.; Riva, A.; Trifiro, F. *Appl. Catal.* **1984**, *9*, 177.

(5) (a) Escardino, A.; Sola, C.; Ruiz, F. *An. Quim.* **1973**, *69*, 385. (b) Centi, G.; Fornasari, G.; Trifiro, F.; *J. Catal.* **1984**, *89*, 44. (c) Hodnett, B. K.; Delmon, B. *Ind. Eng. Chem. Fundam.* **1984**, *23*, 465.

(6) Ai, M. *Bull. Chem. Soc. Jpn.* **1971**, *44*, 761.

(7) Morselli, L.; Trifiro, F.; Urban, L. *J. Catal.* **1982**, *75*, 112.

(8) Bremer, N. J.; Dria, D. US Patent 4 315 864 1982.

(9) (a) Stefani, G.; Fontana, P. US Patents 4 085 122, 4 100 106, 1978. (b) Johnson, J. W.; Jacobson, A. J. Paper presented at the Materials Research Society 1984 Fall Meeting, Boston, p 191.

at 1 atm. Samples were removed from the reservoir in gas-tight syringes and injected through a septum into the reactor containing the β-$(VO)_2P_2O_7$. In experiments involving a mixture of the labeled butanes, a common syringe was used to remove the gases from the reservoirs. The syringe was then thoroughly agitated to assure mixing within the barrel, and half of the mixture was injected into the reactor. The remaining volume was analyzed via mass spectrometry to accurately determine the fraction of each component present.

3. Isotopic Oxygen Studies. $^{18}O_2$ (95 atom % ^{18}O) was placed in a reservoir maintained at 1 atm. Samples were injected via syringe over the catalyst. In one series of experiments, a 7:1 labeled oxygen *n*-butane mixture was prepared by injecting the *n*-butane via a gas-tight syringe into the oxygen-containing reservoir. The mixture was then injected into the reactor in discrete volumes with a syringe.

Maleic Anhydride Experiments. Maleic anhydride was introduced into the reactor via a microliter syringe. The maleic anhydride was melted and a known volume drawn into the syringe needle. The needle was then introduced into the reactor hot zone above the vanadyl pyrophosphate and injected into the He flow.

Effluent Analysis. Condensable products were collected by passing the effluent stream through a 1.6 mm o.d. stainless steel capillary directed to the bottom of a dry ice–isopropyl alcohol bath cooled 4 mm diameter glass tube containing a few hundred milligrams of toluene. A Finnigan automated gas chromatography/El-C1 mass spectrometer system was used to determine the labeling in the products. Noncondensable effluent was collected and analyzed with a Kratos MS 25Q mass spectrometer.

Structural Analysis. X-ray diffraction patterns of the vanadyl pyrophosphates were obtained by using a Rigaku D Max 2A diffractometer. X-band EPR spectra were obtained on powdered samples at room and liquid nitrogen temperatures by using a Varian E1/9 spectrometer. Infrared spectra of β-$(VO)_2P_2O_7$ were obtained from Nujol mulls on a Nicolet 5SX spectrometer.

Results and Discussion

Catalyst Structure. The structure of β-$(VO)_2P_2O_7$ has been the subject of a number of studies,[2b,10] and one crystal structure determination[11] has appeared. Slow cooling of a sample of β-$(VO)_2P_2O_7$, prepared in our laboratory, from 1000 °C allowed the isolation of a diffractable crystal on the order of 0.2 mm on a side. Unit cell and space group determinations on the crystal supported the gross structure previously reported,[11] and the refined structure was not further pursued.[12] β-$(VO)_2P_2O_7$ contains double chains of edge-sharing VO_6 octahedra linked by pyrophosphate units. The pairs of edge-bridged octahedra are linked into a chain through the axial oxygens. This structure contains proximate vanadium centers on all the crystal faces, which could be important for the multielectron redox reactions the catalyst performs. The crystal structure also indicates that the axial vanadium–oxygen bond lengths within an octahedra are not equivalent. One of the vanadium–oxygen bonds can be viewed as a vanadyl group (V=O), while the other interaction is a weaker Lewis acid–base interaction (V=O → V=O). This tetragonal distortion of the octahedral environment would be expected to result in a singly degenerate ground state (B_2) relatively free of spin–orbit contributions from the excited state (E). β-$(VO)_2P_2O_7$ exhibits a broad but intense EPR signal at room temperature, reflecting the nondegeneracy of the ground state and a magnetically concentrated nature of the composition (Table II).

Since vanadyl pyrophosphate contains proximate vanadium centers, which are axially and edge-bridged to each other, spin–spin coupling between the electrons might be expected. The interaction might occur via direct overlap of vanadium orbitals containing the unpaired spin density or indirectly through the bridging oxygen atoms (superexchange). Most of the EPR signal intensity observed likely results from isolated spin centers formed on the conversion of $(VO)HPO_4 \cdot 0.5H_2O$ to the pyrophosphate.[9b] The broad EPR line of the material brought to steady state in the butane/O_2 reaction precludes the definitive identification of a half-field ($\Delta m_s = 2$) transition indicative of a triplet state resulting from antiferromagnetic coupling of the spins on proximate vanadyl groups.

(10) Bordes, E.; Courtine, P. *J. Catal.* **1979**, *57*, 236.
(11) Gorbunova, Y. E.; Linde, S. A. *Sov. Phys.*—Dokl. *Engl. Transl.* **1979**, 24, 138.
(12) Crystals grown and analyzed by Prof. Edward Kostiner of the University of Connecticut.

Table II. EPR Data[a] of β-$(VO)_2P_2O_7$ Samples[b]

sample	sig center, G	*g* val	normalized intensity[c]
freshly calcined	3256	1.97	0.83
	1625	3.93	1.7×10^{-3}
reaction equil	3256	1.97	1.00
microreact reduced[d]	3256	1.97	1.02
microreact oxidized[e]	3256	1.97	0.98

[a] Spectrometer frequency = 9.02×10^9 Hz, power = 2 mW, scan rate = 2 min. [b] Particles, 10–30 mesh. [c] All areas normalized to that of butane–air reaction equilibrated sample. [d] Equilibrated catalyst was pulsed at 400 °C with butane until constant butane breakthrough was observed. [e] Equilibrated catalyst was pulsed at 400 °C with O_2 until constant O_2 breakthrough was observed.

However, the freshly calcined β-phase contains approximately 20% V(V) and exhibits a much sharper EPR signal, which allows the identification of the weak half-field transition. This evidence of the population of the triplet state at room temperature indicates that a significant electronic interaction between vanadium centers exists, perhaps providing an effective electron shuttle pathway at the temperatures where butane oxidation takes place.

The role of the lattice oxygen in the oxidation of butane can be studied on the basis of the relative amounts of surface vanadium atoms and subsurface or bulk, vanadium centers. From the experimental skeletal density (3.07 g/cm^3), the volume occupied by a formula unit of vanadyl pyrophosphate can be determined. When this volume and the surface area (17.1 m^2/g) of prepared material are used, an estimate of 1.10×10^{20} V surface atoms/g (1.8×10^4 mol/g) is calculated. One gram of β-phase contains 3.91×10^{21} V atoms (6.5×10^{-3} mol), and thus approximately $^1/_{36}$ of the vanadium is at the surface in the catalyst. If the catalytic activity arises from only oxygen associated with the surface, the process should be distinguishagble from one associated with a traditional Mars–van Krevelen mechanism where bulk redox reactions of the metal oxide take place.

Pulse Redox Studies. It should be possible to independently study the two catalyst redox steps associated with a Mars–van Krevelen mechanism by using a pulse reactor. In a first step, oxidant can be pulsed over the catalyst to fully oxidize it, and then in a second step, the reductant can be pulsed over the catalyst to undergo reaction. Should only labile surface physisorbed oxygen be involved in the reaction over β-$(VO)_2P_2O_7$, no net oxygen uptake or butane oxidation would be observed. If the vanadyl pyrophosphate can be cycled between reduced and oxidized states, butane reaction and oxygen uptake will serve as measures of the involvement of chemisorbed and bulk lattice oxygen in the process.

The pulse microreactor studies carried out involved the use of 0.5 g of β-$(VO)_2P_2O_7$ which had been brought to a steady state in the conintuous butane oxidation reaction (see Experimental Section). The pulse experiments involved treating the catalyst with oxygen (1.90×10^{-5} mol of O_2 per pulse) at 400 °C until constant O_2 breakthrough was observed. This constant breakthrough of O_2 was indistinguishable from the amount of O_2 fed in the pulse within experimental error and thus represented very little or no further oxidation of the solid. The vanadyl pyrophosphate was then pulsed with 1.78×10^{-5} mol of butane, and the effluent gases were analyzed. Following a number of pulses, the catalyst was reoxidized to constant O_2 breakthrough.

The selectivities observed from the butane conversion were in the 40–50% range for maleic anhydride with the balance to combustion products (Figure 1). Intermediate oxidation products such as butenes, butadiene, crotonaldehyde, or furan were not detected in the effluent from the butane pulses. The lack of formation of intermediate oxidation products over vanadyl pyrophosphate is significant when contrasted with previous studies of olefin oxidation over VPO_x phases.[4,6,7]

The reoxidation of the catalyst always resulted in the production of some CO and CO_2 in the effluent of the first few oxygen pulses. Analysis of the products from the reoxidation process showed that no maleic anhydride or other noncombustion products were being formed. This result indicated that not all of the butane pulse was

Table III. Butane and O_2 Redox Pulse Cycle Products and Oxygen Balance

butane pulses[a]						oxygen pulses[b]			
no. of pulses	CO, mol × 10^8	CO_2, mol × 10^8	MA,[c] mol × 10^8	O_2 loss,[d] mol × 10^8	O_2 loss coke cor,[e] mol × 10^8	no. of pulses[f]	equiv, mol × 10^8	O_2 uptake, mol × 10^8	balance[g]
1	171	556	307	2176	2114	15	61	2042	+3.5
2	209	638	424	2757	2662	14	95	2543	+4.8
4	221	707	514	3197	3042	13	155	3047	−0.1
5	247	792	554	3509	3362	17	146	3334	−0.8
8	294	883	590	3764	3518	14	246	3890	−9.6

[a] 1.78×10^{-5} mol of butane per pulse. [b] 1.91×10^{-5} mol of O_2 per pulse. [c] Maleic anhydride. [d] O_2 loss is equal to $1.125CO + 1.625CO_2 + 3.5MA$ to include the water formed during butane oxidation. [e] Coke calculated from the CO_2 and C produced during the O_2 pulse sequence is deducted from the O_2 loss value. [f] Oxygen pulses were continued until constant O_2 breakthrough was firmly established. [g] Balance is a percent calculated from $(\{[O_2 \text{ loss (cor)}] - [O_2 \text{ uptake}]\}/[O_2 \text{ loss (cor)}]) \times 100$.

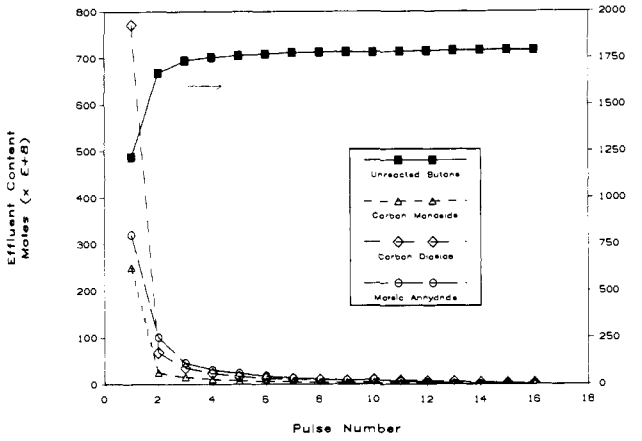

Figure 1. Effluent product distribution as a function of pulse number for 1.78×10^{-5} mol butane pulse (lag time between pulses of 6 min) over 0.5 g of β-$(VO)_2P_2O_7$ at 400 °C. Left vertical axis is for product amounts, right vertical axis for the amount of unreacted butane.

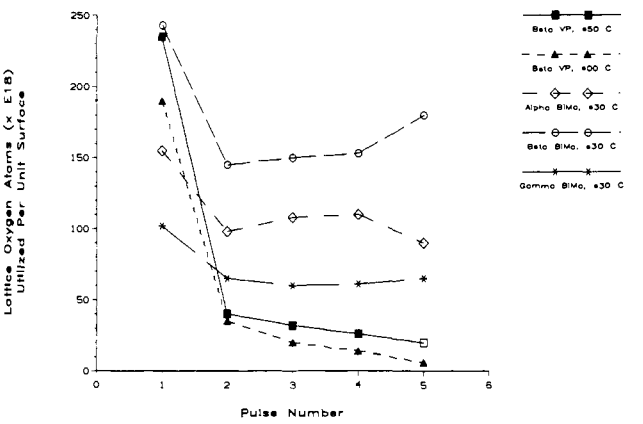

Figure 2. Contrast in the oxidative capacity of β-$(VO)_2P_2O_7$ and bismuth molybdates. Bismuth molybdate data are for the ammoxidation of propylene in the absence of O_2[15] (6.7 μmol of propylene and 13.5 μmol of ammonia per pulse). Lattice oxygen utilization on the vertical axis is in units of oxygen atoms ($\times 10^{18}$) per unit of surface area (m^2). Beta VP refers to β-$(VO)_2P_2O_7$, alpha BiMo to α-$Bi_2Mo_3O_{12}$, beta BiMo to β-$Bi_2Mo_2O_9$, and gamma BiMo to γ-Bi_2MoO_6.

being converted to products volatile at 400 °C. Knowing the nature of the adsorbed carbon-containing species is necessary in order to calculate a complete oxygen balance for the redox cycle.[13] Table III contains data from a series of cycles involving different numbers of butane pulses. As the activity quickly dropped and the catalyst became more and more reduced, the amount of carbon-containing material that remained on the catalyst increased and made it more difficult to close the oxygen balance. The balances were calculated based on the assumption that the combustion products observed during reoxidation originated from C (coke) present on the catalyst surface. As can be seen in the table, balances within ±5% can be achieved through a five butane pulse experiment with this assumption. As reduction proceeds, the assumption most likely breaks down as a result of the adsorbed material becoming more hydrocarbon in nature. The inability to specifically assign the extent of oxidation of the hydrocarbon adsorbed during long butane pulse sequences makes it very difficult to close an oxygen balance for the vanadyl pyrophosphate upon reoxidation.

The data in Table III and Figure 1 both indicate a limited oxidation capacity associated with β-$(VO)_2P_2O_7$. The activity for butane oxidation falls off rapidly, and indicates that approximately 7.0×10^{-5} mol of equiv O_2 is available per gram of β-phase. This value approaches an equivalence of one oxygen atom per surface vanadium atom (1.8×10^{-4} mol/g). This restricted participation of lattice oxygen is in sharp contrast to the behavior of other metal oxide redox catalysts as is illustrated in Figure 2. Bismuth molybdate has been shown to undergo bulk reduction by propylene both in oxidation[14] and ammoxidation[15] reactions, thus exhibiting significant oxidation activity through many pulses of the hydrocarbon. Oxides which exhibit bulk reduction have been shown to undergo changes in activity as a function of intervening time between pulses of reductant. As seen in Figure 3, the variation in the intervening time between butane pulses from 6 to 1.5 min has little or no effect on the observed butane conversion. Therefore, the reordering of lattice oxygen is not important to the observed activity at least on the order of a minute.

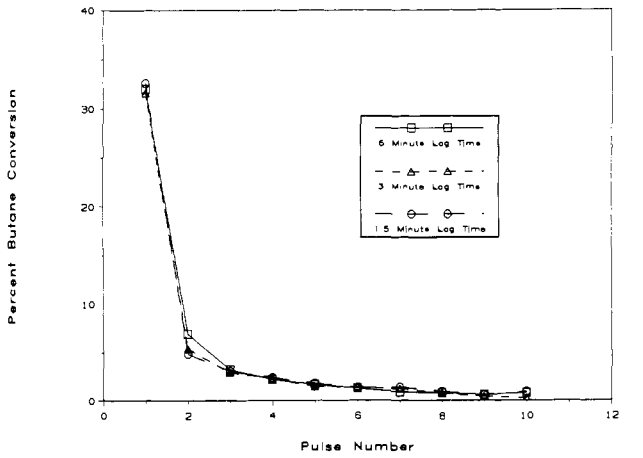

Figure 3. Butane conversion per pulse (1.78×10^{-5} mol) in the absence of O_2 for various lag times between pulses.

Support for essentially no change in the redox state of vanadium in the bulk β-phase in going from the oxidized to the reduced state in the pulse reactor at 400 °C comes from the EPR spectra. As seen in Table II, little change in intensity is observed between the butane reduced and the reoxidized catalyst.

The reoxidation of the vanadyl pyrophosphate surface after the multipulse butane experiments produced significant amounts of

(13) Similar behavior has been observed with xylene oxidation over V_2O_5–TiO_2 and has been assigned to the formation of polymeric material: see Bond, G. C.; Konig, P. *J. Catal.* **1982**, *77*, 309.

(14) (a) Keulks, G. W. *J. Catal.* **1970**, *19*, 232. (b) Krenzke, L. D.; Keulks, G. W. *J. Catal.* **1980**, *61*, 316.

(15) Brazdil, J. F.; Suresh, D. D.; Grasselli, R. K. *J. Catal.* **1980**, *66*, 347.

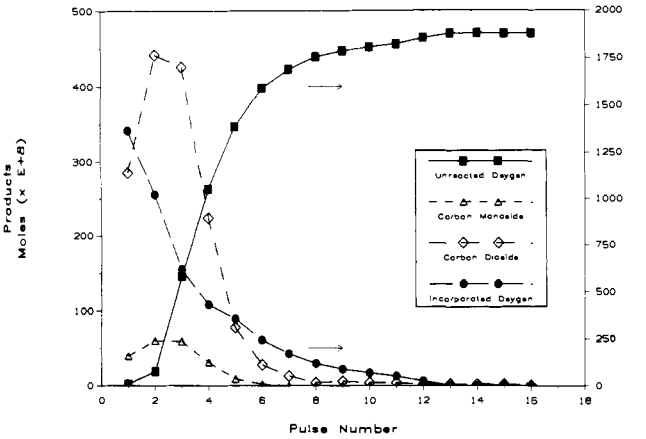

Figure 4. Product distribution as a function of pulse number for 1.91×10^{-5} mol oxygen pulses over 0.5 g of β-$(VO)_2P_2O_7$ at 400 °C. Left vertical axis is for product amounts, right vertical axis for amounts of incorporated and unreacted oxygen.

CO and CO_2 as mentioned previously. Interestingly, the amount of combustion products maximized in the effluent only after a few pulses as is seen in Figure 4. This behavior may indicate a stepwise process for the removal of the "coke" where first the catalyst surface is reoxidized (vide infra).

Reaction Order Studies. The pulse redox studies indicate that the oxidation of butane over vanadyl pyrophosphate can be broken into two general steps:

$$R + M\text{-}O_x \rightleftharpoons R\text{-}O_x + M \quad (a)$$

$$M + O_2 \rightleftharpoons M\text{-}O_x \quad (b)$$

This process is that proposed by Mars and van Krevelen for metal oxides capable of undergoing bulk redox processes and exhibits the general rate expression

$$\text{rate} = r_R = \frac{k_o k_r p_o p_r}{k_o p_o + n k_r p_r} \quad (1)$$

which has an equivalent form

$$r_R = \frac{1}{\frac{1}{k_r p_r} + \frac{n}{k_o p_o}} \quad (2)$$

where r_R = hydrocarbon reaction rate, k_r = reaction reaction constant, k_o = specific rate of O_2 absorption, p_o = partial pressure of O_2, p_r = partial pressure of hydrocarbon, and n = stoichiometric number of moles of O_2 required for the reaction.

In expression 2, if the reaction rate (or adsorption) of the hydrocarbon with the surface is slow with respect to the reoxidation of the catalyst (or adsorption of O_2), the rate reduces to being equal to $k_r p_r$. If the reaction of the surface with O_2 is slow relative to the adsorption or reaction of R, the rate expression becomes $k_o p_o/n$ or $k'_o p_o$.

For the oxidation of aromatics to maleic anhydride over vanadium-containing catalysts, the rates of hydrocarbon oxidation and readsorption of O_2 are comparable and the general expressions 1 or 2 apply. The same expressions were found to apply to the oxidation of butane over VPO_x catalysts by Escardino et al.[5a] In steady-state operation, the value of p_o is usually high, and thus the rate of regeneration of the catalyst with O_2 is faster than the reaction (adsorption) of butane, and the rate expression reduces to $k_r p_r$.

Although the pulse microreactor operated in a reduction or oxidation cycle cannot properly determine the rate constants and orders for continuous processes, it can be used to study the catalyst oxidation and reduction reactions [(a) and (b)] for the vanadyl pyrophosphate independently of each other for pulse cycles with butane and oxygen, respectively. In studying the dependence of the reactions on p_o and p_r exclusive of one another, the situation is complicated in that the vanadyl pyrophosphate is no longer a catalyst but a reagent. A general expression for the reaction of the oxidized catalyst with butane is

$$r_{red} = k_{red}[C_4H_{10}]^j[VPO_{ox}]^k \quad (3)$$

where $[VPO_{ox}]$ is the concentration (distribution) of the reactive oxygen on the surface. The values of k and $[VPO_{ox}]$ may depend on the stoichiometry of the reaction with butane. The reaction of the reduced catalyst could be generally characterized as

$$r_{ox} = k_{ox}[O_2]^l[VPO_{red}]^m \quad (4)$$

where $[VPO_{red}]$ is the concentration (distribution) of vacancies which can absorb or react with O_2. In the limit where the concentration of redox sites associated with the vanadyl pyrophosphate are in large excess over the amount of reactant gas, the expressions 3 and 4 reduce to

$$r_{red} = k'_{red}[C_4H_{10}]^j \quad (5)$$

$$r_{ox} = k'_{ox}[O_2]^l \quad (6)$$

The values of j and l can be investigated in the pulse reactor by varying the concentration of the reactant in the pulse at a constant contact time by using the differential method.[16] Plots of the log of the amount of a pulse reacted vs. the original reactant quantity in the pulse yields the values of j and l, with the y intercept being the log of the apparent rate constant (k').

The results of experiments using concentrations of 1.00, 0.50, 0.25, and 0.10 volume fractions of butane in the pulse appear in Table IV for the conversion of the initial pulse over the reoxidized catalyst and for the $[(1/2x) + 1]$th pulse of each sequence where x is the volume fraction of butane in the pulse. The reactivity over the fully oxidized catalyst exhibits a slope of 0.71 as a result of the significant changes in $[VPO_{ox}]$ at high butane concentrations in the pulse. The requirement of between 3.5 and 6.5 equiv of O_2 for each butane molecule reacted makes the surface distribution and concentration of $[VPO_{ox}]$ relevant. At the low butane concentrations, conversions are very high, thus bringing large uncertainties into the differential analysis. The data for the $[(1/2x) + 1]$th pulses from the 0.50, 0.25, and 0.10 volume fractions of butane experiments indicate a more linear slope, with the data from the 0.25 and 0.10 volume fraction pulses fitting a first-order reaction in butane very well.

The data for the initial and $[(1/2y) + 1]$th oxygen pulses (y is the volume fraction of oxygen in the pulse) over the reduced catalyst appear in Table V and also indicate a first-order reaction.

Table IV. Determination of Butane Reaction Order with β-$(VO)_2P_2O_7$ at 400 °C by Differential Method

x^a	$C_o{}^b$	$C_r{}^c$	log C_o	log C_r
		Initial Pulse Conversion		
1.00	1780	890	3.25	2.95
0.50	890	615	2.95	2.79
0.25	445	399	2.65	2.60
0.10	178	173	2.25	2.24
	line regres anal.			
	all concn		0.71 slope[d]	0.992 correlation
	three lowest concn		0.79 slope[d]	0.995 correlation
		$[(1/2x)^a + 1]$th Pulse Conversion		
0.50	890	193	2.95	2.29
0.25	445	135	2.65	2.13
0.10	178	54	2.25	1.73
	lin regres anal.			
	all concn		0.81 slope[d]	0.988 correlation
	two lowest concn		0.99 slope[d]	−0.630 intercept

[a] x is the volume fraction of butane in the pulse. [b] Amount of butane in pulse (mol × 10^8); helium makes up balance of pulse. [c] Butane converted (mol × 10^8). [d] Slope gives apparent reaction order; see text for explanation of values.

(16) Pilling, M. J. "Reaction Kinetics"; Clarendon Press: Oxford, 1975; p 7.

Table V. Determination of Oxygen Reaction Order with β-$(VO)_2P_2O_7$ at 400 °C by Differential Method

y^a	C_o^b	C_r^c	log C_o	log C_r
1.00	1847	1213	3.27	3.08
0.51	938	847	2.97	2.93
0.29	529	519	2.72	2.72
0.14	259	258	2.41	2.41
	lin regres anal.			
	all concn		0.79 slope[d]	0.989 correlation
	three lowest concn		0.93 slope[d]	0.999 correlation
pulse no.	C_0	C_r	log C_0	log C_r
	[(1/2y) + 1]th Pulse Conversions			
2	1847	373	3.27	2.57
3	938	217	2.97	2.34
5	527	113	2.72	2.05
8	259	61	2.41	1.78
	lin regres anal.			
	all concn		0.94 slope[d]	0.997 correlation
	three lowest concn		1.00 slope[d]	0.997 correlation

[a] y is the volume fraction of oxygen in the pulse. [b] Amount of O_2 in pulse (mol × 10^8); helium makes up the balance of the pulse. [c] O_2 converted (mol × 10^8). [d] Slopes gives apparent reaction order; see text.

Table VI. Determination of Oxygen Reaction Order with β-$(VO)_2P_2O_7$ at 400 °C by Differential Method (Combustion Product Free Data)[a]

y^a	C_0^c	C_r^d	log C_0	log C_r
	Initial Pulse Conversions			
1.00	1847	1033	3.27	3.01
0.51	938	728	2.97	2.86
0.29	527	456	2.72	2.66
0.14	259	226	2.41	2.35
	lin regres anal.			
	all concn		0.77 slope[e]	0.988 correlation
	three lowest concn		0.91 slope[e]	0.998 correlation
pulse no.	C_o	C_r	log C_o	log C_r
	[(1/2y) + 1]th Pulse Conversions			
2	1847	343	3.27	2.54
3	938	202	2.97	2.31
5	527	109	2.72	2.04
8	259	57	2.41	1.76
	lin regres anal.			
	all concn		0.92 slope[e]	0.998 correlation
	three lowest concn		0.98 slope[e]	−0.607 correlation

[a] The oxygen in observed CO_2 and CO was fractioned out. [b] y is the volume fraction of oxygen in the pulse. [c] Amount of O_2 in pulse (mol × 10^8); helium makes up the balance of the pulse. [d] O_2 converted (mol × 10^8). [e] Slope gives apparent reaction order; see text.

The reoxidation of the reduced catalyst also involved the removal of adsorbed material. This combustion reaction may proceed with a different reaction order with respect to oxygen partial pressure than the reoxidation of the catalyst. Thus, data with the amount of oxygen involved with the conversion of surface "coke" to CO and CO_2 factored out for each pulse appear in Table VI and clearly show that the reoxidation of the vanadyl pyrophosphate is first order in oxygen. This result indicates that a reaction such as $O_2 + 2M \rightleftharpoons 2O{=}M$ is not rate-determining for the reoxidation of the catalyst, as a reaction order of 0.5 would have been observed as is seen with the oxidation of bismuth molybdates after reduction by propylene and ammonia.[15,17]

The data obtained from the intermediate pulses at low reactant concentrations provide the best information for analysis by the differential method. The y intercept from the butane pulse experiment using the two lowest butane concentrations is −0.63,

Table VII. Mass Spectral Analysis of the Condensable Effluent from the Butane Reaction Over D_2O-Treated β-$(VO)_2P_2O_7$

	MI (m/e 58)	MI + 1 (m/e 59)	MI + 2 (m/e 60)
	C_4H_{10} (Butane) Mass Spectrum		
obsd intens	12530	620	36
rel intens	0.950	0.047	0.003
calcd rel intens[a]	0.954	0.045	0.001
	MI (m/e 98)	MI + 1 (m/e 99)	MI + 2 (m/e 100)
	$C_3H_2O_3$ (Maleic Anhydride) Mass Spectrum		
obsd intens	7	38	86
rel intens	0.053	0.290	0.656
calcd rel intens[b]	0.948	0.044	0.007

[a] Distribution expected for C_4H_{10} based on natural ^2H and ^{13}C abundances. [b] Distribution expected for $C_4H_2O_3$ based on natural ^2H, ^{13}C, and ^{18}O abundances.

resulting in a value of k'_{red} of 0.23. The extent of surface oxidation of the catalyst during these middle pulses indicated that approximately half of the surface vanadium was in an oxidized state. The analysis of the effluent indicated that each butane converted consumed an average of 4.5 equiv of O_2 from the catalyst. These values coupled with the observed k'_{red} result in the calculation of $k_{red} = 2.1[(VPO)_{surf}]$ *on a per O_2 basis*. For the reoxidation of the catalyst, the surface was approximately 35% reduced during the [(1/2y) + 1]th oxygen pulses. This extent of surface oxidation and the calculated k'_{ox} of 0.25 from the y intercept results in a value of $k_{ox} = 0.69[(VPO)_{surf}]$.

The comparison of the two rate constants (on a per O_2 basis) calculated from the pulse studies allows a crude estimation of the relative extent of surface oxidation during continuous operation to be made according to

$$K_{surf\,ox} = \frac{0.69[(VPO)_{surf}][O_2]}{2.14[(VPO)_{surf}][C_4H_{10}]} = 0.33\frac{[O_2]}{[C_4H_{10}]}$$

The relative rates of the surface redox reaction indicate that even at high O_2/C_4H_{10} ratios, a significant concentration of V(IV) is present on the surface of the catalyst.

The EPR and chemical analysis data supporting a V(IV) $\rightleftarrows$ V(V) couple, the observed reversible oxidation capacity approaching one O_2 per two surface vanadium centers, and the first-order reaction of O_2 with the vanadyl pyrophosphate suggest the possible formation of peroxo-bridged vanadium centers as the initially formed complex on the catalyst surface. Recently, a superoxide ion was proposed as the active bound oxygen species for the oxidation of benzene to maleic anhydride over a vanadium-containing catalyst.[18] If superoxide were the predominant oxygen species formed on the surface of β-$(VO)_2P_2O_7$, the reversible oxygen capacity would have been expected to be much higher than that observed during the pulse redox cycles.

Studies with Labeled Compounds. 1. Deuterated Water. Infrared spectra of the reactor-equilibrated β-$(VO)_2P_2O_7$ exhibit adsorptions in the OH stretching region. The observation might be explained in terms of the "capping" of phosphorus and vanadium centers on the surface with OH groups. D_2O was pulsed in large excess at 400 °C over 0.50 g of vanadyl pyrophosphate which had been pulsed with O_2 until constant oxygen breakthrough (near zero uptake) was observed. If the surface contained exchangeable protons or hydrolyzable oxide groups, significant and essentially complete deuteration should have occurred. Butane was then pulsed over the catalyst, and the effluent was trapped in toluene maintained at −78 °C. The effluent was analyzed by GC–mass spectrometry and was determined to contain unreacted butane and product maleic anhydride. The observed mass spectra of these compounds appear in Table VII.

For butane, the observed distribution for the molecular ion (MI), MI + 1, and MI + 2 peaks is very close to the calculated

(17) Grasselli, R. K.; Burrington, J. D.; Brazdil, J. F. *Faraday Disc. Chem. Soc.* **1982**, *72*, 203.

(18) Petts, R. W.; Waugh, K. C. *J. Chem. Soc. Faraday Trans. 1* **1982**, *78*, 803.

values expected for a C_4H_{10} molecule containing natural isotopic abundance. Even if it is assumed that no deviations exist in the experimental method, the maximum extent of deuterium–protium exchange of effluent butane with the surface of the catalyst is 0.03%. These results indicate that butane does not *reversibly* chemisorb with hydrogen exchange onto the surface of the vanadyl pyrophosphate during the oxidation reaction.

When the product maleic anhydride is observed by mass spectrometry, a very large deuterium content is present. As can be seen in Table VII, the bulk of the maleic anhydride contained deuterium, with nearly two-thirds containing two deuterium atoms. This result indicates that every hydrogen present in butane is subject to labilization once the butane is *irreversibly* adsorbed onto the surface. The process of dehydrogenation of the central atoms of butane is obviously not a static one where the remaining hydrogen on each of the carbons is isolated from further reaction (exchange) during the oxidation to maleic anhydride.[19]

The high deuterium content in the maleic anhydride may result from very fast proton (or hydroxyl) exchange/migration on the surface. The exchange reactions may occur fast enough to result in the formation of a pool of protons and deuterons so that a statistical distribution of ^1H and $^2H(D)$ appears in the product maleic anhydride. The 0.50 g of vanadyl pyrophosphate contains approximately 9×10^{-5} mol of vanadium on the surface, with a like number of phosphorus atomic centers. Assuming that every surface V and P is terminated by an OD group after the deuteration of the oxygen-equilibrated catalyst, the surface would contain 1.8×10^{-4} mol of M–OD sites.

The fraction of ^1H in the ^1H–^2H pool is determined by the amount of the butane pulse which undergoes reaction. At the 1-s apparent contact time used in the experiment, 25–27% of the 1.8×10^{-5} mol pulse reacted which represents a proton pool of approximately 4.7×10^{-5} mol. A statistical distribution of ^1H and ^2H in the maleic anhydride from this pool would result in the observation of 4.4% $^1H_2$, 33.2% $^1H^2H$, and 62.4% $^2H_2$ product. This calculated distribution is very similar to that observed experimentally and indicates that migration, exchange, and equilibration of hydrogen on the surface of the catalyst is fast compared to the time for the conversion of adsorbed butane to maleic anhydride. The small "excess" of ^1H in the observed data could result from the incomplete equilibration of the isotope pool or from the incomplete exchange of all the surface P and V sites with D_2O.

Alternatively, the high deuterium content in the maleic anhydride could result from the consecutive desorption–readsorption of the maleic anhydride accompanied by hydrogen exchange at the deuterium–rich readsorption site. In order to get an estimate of this contribution, 4.8×10^{-6} mol of maleic anhydride was pulsed over the oxygen-equilibrated and freshly deuterated vanadyl pyrophosphate. The observed mass spectral data of the effluent maleic anhydride indicated the presence of 82.5% $^1H_2$, 13.8% $^1H^2H$, and 3.8% $^2H_2$ product after correction for naturally occurring isotopic abundances. This result indicates that reversible maleic anhydride adsorption does occur at 400 °C but that hydrogen exchange does not occur to an equivalent extent at both carbons in the adsorbed molecule. If the exchange at both of the carbon centers occurred in the adsorbed species, a skewed distribution would have been observed in the mass spectrum where the unadsorbed maleic anhydride would contain two protons while the material which was adsorbed would be nearly all dideuterated as a result of the large available deuterium pool on the surface. The adsorbed maleic anhydride may be forming a metal alkyl, leading to exchange at only one of the carbons with the observed dideuterated product resulting in part from readsorption of the monodeuterated species as well as sequential multiexchange without desorption. Although there is no way to precisely determine how much of the maleic anhydride did adsorb–desorb from the surface, the relatively low deuterium content indicates that this process is not a major contributor to the extensive exchange observed for the maleic anhydride formed from butane in the previous experiment.

2. Oxygen-Exchange Studies. The exchange of oxygen between the gas phase and the surface is an important consideration in any studies involving oxygen-labeling experiments to determine the significance of whether gas-phase, physisorbed, or lattice oxygen is associated with the reactivity. The pulsing at 400 °C of 1.90×10^{-5} mol of $^{18}O_2$ (95%) over a 0.5 g of β-$(VO)_2P_2O_7$ which had been equilibrated with pulses of natural abundance oxygen resulted in an effluent isotopic distribution ($92 \pm 1\%$ $^{18}O_2$, $5 \pm 1\%$ $^{16}O^{18}O$, and $3 \pm 1\%$ $^{16}O_2$) indistinguishable from that of the feed. The oxygen-equilibrated catalyst does not undergo exchange reactions with the gas phase, thus indicating the irreversibility of the surface reoxidation reaction.

The limited redox capacity of vanadyl pyrophosphate and the multielectron nature of the butane oxidation reaction may indicate that oxygen exchange/migration on the surface of the vanadyl pyrophosphate may be an important factor in its activity. $^{18}O_2$-enriched air (65.5% ^{18}O and 35.5% ^{16}O)/butane mixtures with an effective O_2/butane ratio of 3.5 to 1 were pulsed over the oxygen equilibrated sample at 400 °C. Ten consecutive 0.90-mL pulses each containing 4.9×10^{-6} mol of butane were sent over the catalyst at 5-min intervals, and the effluent was analyzed. Analysis of the gaseous products indicated an average butane conversion of 50%, consuming 4.25 mol of O_2 per mol of butane.

From the butane conversion and oxygen consumption rate, the appearance of oxygen introduced with the pulses into the products can be calculated based on potential pools of exchangeable oxygen in the vanadyl pyrophosphate. Three limiting pools can be considered: (1) Only a single oxygen bound to each surface vanadium can react with butane. The vacancy produced by butane oxidation can only be filled via gas-phase adsorption, and no scrambling with other oxygens in the catalyst occurs. This case is the static limit associated with the V(V) $\rightleftarrows$ V(IV) couple on the surface. For the 0.5 g of material used, this pool is equivalent to 4.5×10^{-5} mol O_2. (2) An intermediate case where the "oxidized" surface layer can be considered equivalent to $(VO)PO_4$ and an oxygen–oxygen exchange reaction occurs quickly on the pulse interval time scale, creating an exchangeable oxygen pool of five O atoms per surface V (2.25×10^{-4} mol of O_2). As vacancies occur in this layer with butane oxidation, O_2 incorporated from the gas phase scrambles with the remaining oxygen atoms in the surface layer. (3) There is an extreme case where all the oxygen in the pyrophosphate sample is in fast exchange with any oxygen incorporated into surface vacancies from the gas phase. This pool would be equivalent to 7.3×10^{-3} mol of O_2 based on $(VO)_2P_2O_7$.

Calculations of the expected pulse originating oxygen content in the products as a function of the air/butane pulse number can be made for the three case models. The calculations made were based on two scenarios: (A) for a given pulse, the butane reacts exclusively with oxygen already present in the catalyst and the oxygen in that pulse reoxidizes the vacancies; and (B) for a given pulse, 90% of the product contains oxygen already present in the catalyst but reoxidation occurs quickly enough such that 10% of the product contains oxygen which was cofed in that particular pulse. The latter scenario was considered as the CO_2 and CO produced from the first pulse contained enough ^{18}O to indicate an approximate 10% incorporation of cofed oxygen into the product. The amount of oxygen in the product originating from the gas-phase oxygen, which reoxidized the catalyst during the pulse sequence, can be calculated for the various models and scenarios. The resulting values, designated as O_{gas}, appear in Table VIII.

The gaseous effluent produced on passing the $^{18}O_2(^{16}O_2)/C_4H_{10}$ mixture over the catalyst at 400 °C was trapped and analyzed by mass spectrometry. While both product CO and CO_2 could be observed, the CO data were significantly complicated by interferences, especially from background air (m/e N_2 28 as is $C^{16}O$). The CO_2 data were only obscured by minor interferences at m/e 44 from butane fragmentation and background air which were factored out in a straightforward manner. The correction amounted to only 10–15% of the observed intensity; thus, the

(19) The oxidation of propylene on bismuth molybdate in the presence of D_2O showed very minor amounts of exchaange. See: Adams, C. R.; Jennings, T. J. *J. Catal.* **1964**, *3*, 549.

Table VIII. O_{gas} Product Content Calculated as a Function of Pulse Number[a]

	static model 1		surface-exchange model 2		tot exchange model 3	
pulse no.	scenario A	scenario B	scenario A	scenario B	scenario A	scenario B
1	0	10.0	0	10.0	0	10.0
2	24.0	28.7	4.6	13.8	0.14	10.12
3	43.0	43.6	9.0	17.4	0.28	10.23
4	57.0	55.2	13.2	20.8	0.41	10.34
5	67.0	64.6	17.2	24.0	0.55	10.46
6	75.0	72.0	21.1	27.3	0.70	10.58
7	81.0	77.8	24.7	30.3	0.84	10.69
8	86.0	82.4	28.2	33.1	0.97	10.80
9	89.0	86.0	31.5	35.9	1.11	10.92
10	92.0	89.0	34.7	38.5	1.25	11.04

[a] Values in percent; see text for detail on models and scenarios.

Table IX. Experimental Results of Passing ^{18}O-Enriched Air/Butane Mixtures Over β-$(VO)_2P_2O_7$ and the Calculation of the Original Gas-Phase Oxygen Content (O_{gas}) in the Product

pulse no.	cor[a] *m/e* 44	raw *m/e* 48	O_{cat} (cor) 44[b]	O_{gas} (cor) 48[b]	$\%O_{gas}$ (cor)
1	26586	115	163.0	16.4	9.1
2	18227	220	134.9	22.6	14.4
3	13764	269	117.0	25.0	17.6
4	15859	664	125.2	39.3	23.9
5	17473	1044	131.1	49.3	27.3
6	14722	1084	120.1	50.3	29.5
7	12736	1084	111.3	54.0	32.7
8	11998	1337	107.8	55.8	34.1
9	14506	2032	118.1	68.8	36.8
10	10104	1542	98.4	59.9	37.8

[a] Mass spectrometry intensity corrected for natural CO_2 presence in air and contributions from background and butane fragmentation. See text. [b] Corrected base on the $^{18}O/^{16}O$ ratio in the air cofed in the butane pulse. See text.

possible errors are relatively small and should not affect the interpretation to a significant degree.

The oxygen isotope distribution in the product CO_2 is expected to be statistical and the distribution resulting from the oxygen originating from the $^{18}O_2$-enriched air (O_{gas}) would be 11.9% $C^{16}O_2$, 45.2% $C^{16}O^{18}O$, and 43.0% $C^{18}O_2$, based on the 65.5% ^{18}O and 34.5% ^{16}O present. The mass spectral data at *m/e* 48 can be exclusively used to calculate the amount of oxygen in the product CO_2 which was originally associated with the air (O_{gas}) fed in the pulses. When this expected distribution and the calculated value of O_{gas} based on the *m/e* 48 peak are used, the amount of oxygen originally associated with the catalyst (O_{cat}) which appears in the product CO_2 can be calculated from the *m/e* 44 mass spectral peak for each pulse. The calculations of O_{gas} and O_{cat} from the experimental results appear in Table IX.

A reasonable fit is obtained for the experimental data with model 2 (scenario B), where all the oxygen atoms in the surface layer can equilibrate with each other (Figure 5). The curvature in the exptl. data could result from a slow oxygen exchange between the surface and subsurface layers. As a test for surface-to-bulk oxygen exchange in the vanadyl pyrophosphate, a redox cycle with butane and labeled O_2 was performed.

$^{16}O_2$ (natural abundance) pulse-equilibrated β-$(VO)_2P_2O_7$ (0.5 g) was pulsed with butane at 400 °C until the butane breakthrough was constant, indicating the removal of $\sim 4.5 \times 10^{-5}$ mol equiv of O_2 from the surface. Some of the removed oxygen may have been associated with partially oxidized material which remained on the surface, but it is considered as being at least partially severed from the vanadium, as a result reducing the O/V ratio from 5 to 4. The catalyst was then reoxidized to constant oxygen breakthrough with $^{18}O_2$ (95%), at which point the surface layer should contain 81% ^{16}O and 19% ^{18}O. The vanadyl pyrophosphate was then immediately pulsed with butane and the gaseous effluent analyzed by mass spectrometry. The CO and CO_2 exhibited an ^{18}O content of 19 ± 1%, giving additional support for the rapid exchange/migration of the surface layer oxygen species.

The sample of vanadyl pyrophosphate was then purged of ^{18}O by cycling through three series of butane and $^{16}O_2$ pulses. The catalyst was then rereduced with butane followed by reoxidation with $^{18}O_2$ (95%) to constant oxygen breakthrough. The oxidized catalyst was then left for 18 h at 400 °C under a flow of He. The catalyst was then pulsed with butane and the CO and CO_2 were found to contain 14 ± 1% ^{18}O. This result indicates that less than a third of the ^{18}O incorporated into the surface layer had diffused into the bulk via exchange. The rate of surface to bulk oxygen exchange is much slower than the dynamic exchange observed within the surface layer. This observation substantiates the very limited participation of subsurface β-$(VO)_2P_2O_7$ in the redox process, as well as suggests an image of a very active surface which can shuttle hydrogen and oxygen species to and away from even a firmly adsorbed intermediate.

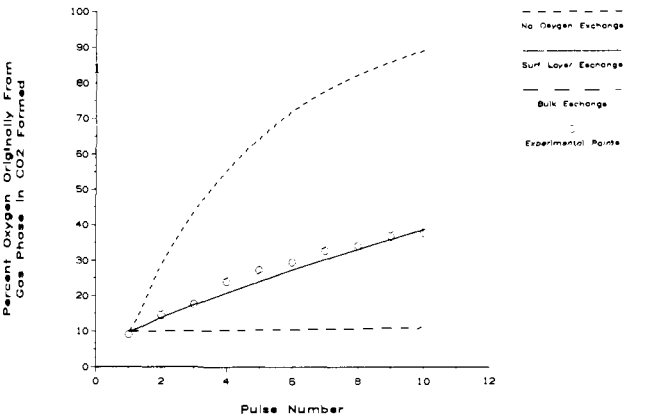

Figure 5. Observed and predicted O_{gas} content vs. pulse number. The "No Oxygen Exchange" line represents model I, scenario B, "Surf Layer Exchange" represents model II, scenerio B, and "Bulk Exchange" represents model III, scenerio B from Table VIII. The experimental points are the $\%O_{gas}$(corr) values from Table IX.

3. Adsorbed Species Oxidation. As the surface of vanadyl pyrophosphate becomes depleted of oxidation capacity, adsorbed carbonaceous materials begin to build up (vide supra). Analysis of the effluent produced on the reoxidation of the catalyst indicated that only combustion products were produced. Since nonselective oxidation takes place, it is of interest whether the material is directly oxidized by gas-phase oxygen or if a sequential oxidation of the surface vanadium and then the carbonaceous species occurs. As mentioned above, the CO and CO_2 produced upon reoxidation after reduction by multiple butane pulses maximized only after two or three pulses of O_2, supporting the sequential reaction scheme.

Reoxidation of the catalyst with $^{18}O_2$ (95%) could give information as to the nature of the adsorbed material and the mechanism of oxidation. If the CO and CO_2 produced contain 95% ^{18}O, then direct oxidation of the carbonaceous material from the gas phase is taking place. ^{18}O (19%) would be expected if the carbonaceous material contained exclusively carbon and hydrogen, and oxidation took place only after significant reoxidation of the surface vanadium. If the adsorbed species contained a significant amount of oxygen and initial reoxidation of the surface takes place, then a value for ^{18}O below 19% would be observed. The CO and CO_2 produced during such an experiment contained 13 ± 1% ^{18}O,

Table X. Kinetic Isotope Effects Calculated from Competitive Experiments Using Butane Mixtures at 400 °C

components	convers	C_x[b]	C_y	C_x^{eff}	C_y^{eff}	X[c]	Y	k_H/k_D
$CH_3CH_2CH_2CH_3(x)$ $CH_3CD_2CD_2CH_3(y)$	27.5	0.500	0.500	0.429	0.571	18.9	8.67	2.18
$CH_3CH_2CH_2CH_3(x)$ $CD_3CH_2CH_2CD_3(y)$	30.4	0.503	0.497	0.498	0.502	15.6	14.7	1.05
$CD_3CH_2CH_2CD_3(x)$ $CH_3CD_2CD_2CH_3(y)$	27.3	0.421	0.579	0.353	0.647	16.5	10.8	2.11

[a] Percent of total butane converted. [b] C_x and C_y are the fractions of the x and y components in the feed; C_x^{eff} and C_y^{eff} are the respective fractions in the efficient. [c] x and y are percents of each isotope represented in the total butane conversion.

suggesting that the adsorbed species is significantly oxidized and that the combustion of this material is preceded by the reoxidation of the catalyst surface. A significant implication of these results is that, like the hydrogen species mobility, the migration/exchange of the oxygen-containing species in the surface layer is fast on the time scale for the conversion of butane and intermediates to products.

4. Deuterated Butane Studies. Previous studies[5] of maleic anhydride formation over VPO_x catalysts have interpreted the results in terms of parallel reaction pathways for the formation of desired maleic anhydride and the unwanted waste (CO, CO_2). The selectively of the overall reaction is controlled by whether the hydrocarbon is activated at a selective (maleic) or nonselective (combustion) site on the surface of the catalyst. If C–H bond breaking is important in butane activation, the presence of a primary kinetic isotope effect in the rate-determining step for the butane oxidation could shed light on the relationship between the maleic anhydride and waste-producing reactions. If parallel reaction pathways are active, the kinetic isotope effect as a function of the position of deuterium substitution in the butane in all probability will be different for the two reaction paths. If selective activation of butane results in eventual production of maleic anhydride, a specific isotope effect may be observed. A parallel nonseletive route to combustion products might exhibit a mixed isotope effect as a function of the statistical amount of ^1H and ^2H present. The overall net effect from the two parallel reactions could be an intermediate, and possibly variable, value for the kinetic isotope effect. If both reactions proceed through the same transition state where C–H bond activation is involved, a very definitive overall isotope effect would be observed as a function of which carbons of butane are deuterated.

The value of $\delta\Delta G^{\ddagger}$ for the cleavage of a C–^{1}H(C–H) vs. a C–^{2}H(C-D) bond of an sp^3-hybridized carbon is approximately 365 cm^{-1} (1.05 kcal).[20] This energy difference would be the maximum expected to be observed if complete breaking of the C–H(D) bond were occurring in the transition state with little or no concomitant making of another bond. This energy difference would lead to a maximum expected value of 2.27 for k_H/k_D at 400 °C if C–H(D) bond cleavage is rate-determining.

In the experiments, a direct competition of one labeled butane against another differently labeled butane was observed by injecting a mixture of approximately equal concentrations over the oxygen-equilibrated vanadyl pyrophosphate at 400 °C. If a specific isotope effect is present, the reaction selectivities for the two butanes should be different. For instance, if a labeled butane (C_D) and an unlabeled butane (C_H) were reacted, the selectively of reaction for each butane would be given by

$$S_H = \frac{k_H[C_H]}{k_H[C_H] + k_D[C_D]}$$

$$S_D = \frac{k_D[C_D]}{k_H[C_H] + k_D[C_D]}$$

During reaction over the catalyst, the selectivities for each isomer should change as the concentrations change if a discrimination for one compound over the other exists. If the compounds react at different rates, the change in the concentration values will not be proportional to each other as the reaction proceeds. As an approximation, the concentration ratio of the reactants in the pulse is assumed to be constant through the reactor bed, and thus the initial concentration of each component can be used as a basis for calculating k_H/k_D. A large kinetic isotope effect would be underestimated if the approximation of constant concentration ratios is inaccurate.

A portion of each mixture was analyzed by mass spectrometry before the balance was injected over the catalyst so that the initial feed molecular ion intensities could be determined. Analysis of the effluent by mass spectrometry indicated the relative intensities of the unreacted butanes. Adjustment of the intensities observed with the ionization/fragmentation sensitivity factor for each of the butanes resulted in the determination of the relative concentrations in the feed and the effluent. The overall conversion of the butane in the experiments was determined by GC analysis. When the conversion and relative concentration data for the feed and effluent are used, the observed kinetic isotope effect for each experiment can be calculated. The ratio of the relative amounts of each butane reacted gives the value of k_H/k_D. For each experiment, two linearly independent equations can be generated for the amount of unlabeled butane (x_H) and the amount of the labeled butane (x_D) reacted

$x_H + x_D$ = tot butane converted (fraction of feed amount)

and

$$\frac{(C_H - x_H)}{(C_H - x_H) + (C_D - x_D)} = C_{H(eff)}$$

where C_H is the fraction of unlabeled butane in the feed, C_D is the fraction of labeled butane in the feed, and $C_{H(eff)}$ is the fraction of unlabeled butane in the effluent. The determination of x_H and x_D allows the calculation of $(x_H/C_H)/(x_D/C_D)$ which is the k_H/k_D value.

Table X contains the results and the reaction rate ratio (k_H/k_D) calculations from experiments involving competitive reactions of $CH_3CH_2CH_2CH_3/CH_3CD_2CD_2CH_3$, $CH_3CH_2CH_2CH_3/CD_3CH_2CH_2CD_3$, and $CD_3CH_2CH_2CD_3/CH_3CD_2CD_2CH_3$ at 400 °C. As can be seen, $CH_3CD_2CD_2CH_3$ reacts at about half the rate of either $CH_3CH_2CH_2CH_3$ or $CD_3CH_2CH_2CD_3$. This observation shows that the rate-determining step for the reaction of butane is the activation of a methylene carbon–hydrogen bond. The magnitude of the isotope effect indicates nearly exclusive reaction via this path, and the transition state involves severing of the C–H(D) bond. A very slight isotope effect is observed in the reaction of $CD_3CH_2CH_2CD_3$, indicating that less than 5% of the butane reaction proceeds by methyl C–H(D) activation. Since the observed selectivity to combustion products from butane is greater than 50% in the reaction, nonselective C–H bond scission cannot account for even a significant fraction of the carbon oxides observed. The isotope effects observed strongly indicate that butane proceeding both to maleic anhydride and combustion products goes through the same rate-determining step. Thus, the selectivity of the reaction is determined during the fast steps after the initial C–H bond activation, and the factors affecting selectivity cannot be determined by studying the kinetics of the butane oxidation.

Propylene oxidation catalysts, such as bismuth molybdate, exhibit similar kinetic isotope effects for allylic C–H bond cleavage to those observed for the butane oxidation over β-$(VO)_2P_2O_7$.[15] Bismuth molybdate will not selectively oxidize saturated hydrocarbons as does the pyrophosphate and reacts much more rapidly

(20) Adler, R. W.; Baker, R.; Brown, J. M. "Mechanism in Organic Chemistry"; Wiley-Interscience: London, 1971; p 14.

with oxygen when reduced than it does with olefin when oxidized.[21] While both catalysts contain M=O or M—OH groups on the surface under reaction conditions, as shown in this work, vanadyl pyrophosphate contains a high concentration of V(IV) centers in the surface layer even in the presence of excess oxygen. The presence of the V(IV) at the surface may be the key to the selective activation and oxidation of butane.

V(IV) may be simply viewed as a transition-metal radical,[22] exhibiting reactivity similar to the more traditional radicals used in organic chemistry for paraffin reactions. The selectivity of bromine atom for hydrogen abstraction from a secondary carbon vs. a primary carbon at 400 °C would be similar to the selectivity observed for the methylene C–H bond activation by vanadyl pyrophosphate. Radical species present on the surface of the catalyst in addition to V(IV), which might be responsible for butane activation, include O_2^-, O_2^{2-}, and O^-. At 400 °C, the highly reactive O^- would be expected to show selectivity for the C–H bonds only in a statistical sense,[23] just as does the fluorine atom. The other oxygen-centered radicals would also exhibit high reactivity, showing a minor selectivity for methylene C–H cleavage. V(IV), with its d orbital based unpaired electron is much less reactive and would be expected to discriminate between the methylene and stronger methyl C–H bonds.

While the activation of the butane occurs through cleavage of a C–H bond, the irreversibility noted in the catalyst deuteration experiments indicates that further reaction takes place on the surface and not in the gas phase. The existence of proximate vanadium centers in the structure allows the instantaneous capture of both species from a homolytically cleaved C–H bond. The C_4H_9 fragment is then oxidized to form maleic anhydride or waste.

Conclusion

The β-$(VO)_2P_2O_7$ phase catalyzes the oxidation of butane to maleic anhydride via redox reaction of its surface layer in a manner kinetically consistent with the Mars–van Krevelen model. The Mars–van Krevelen model has been traditionally used to describe the behavior of metal oxide catalysts which utilize bulk, lattice oxygen in their redox cycle, and thus β-$(VO)_2P_2O_7$ with its surface layer limited reactions is a distinct and exceptional case. The stability of V(IV) within the pyrophosphate structure results in the material's limited oxidation capacity toward hydrocarbons in the absence of oxygen and its resistance to bulk oxidation in the presence of excess oxygen at high temperatures. The surface layer can be oxidized to an extent to V(V), which provides the capacity to oxidize adsorbed hydrocarbons.

V(IV) at the surface of the vanadyl pyrophosphate is proposed not only to activate molecular oxygen but also to be instrumental in the selective activation of the C–H bonds in saturated hydrocarbons. For butane, the activation of the C–H bond at a methylene carbon is the rate-determining step in the oxidation reaction. This high-temperature discrimination between C–H bonds of sp^3-hybridized carbons is a very unique property of β-$(VO)_2P_2O_7$ as an oxidation catalyst. Vanadium(V) present in the vanadyl pyrophosphate surface provides the oxidative capacity to convert the activated butane to products, vs. providing both activation and oxidation functions.[5c] The selectivity of the reaction to maleic anhydride or combustion products is determined after the rate-controlling step and may simply involve the ratio of reaction rates for maleic anhydride desorption from the catalyst surface and further oxidation of maleic anhydride to CO, CO_2, and H_2O.

The results of the redox capacity and labeled compound experiments shed light on the ways in which a simple metal phosphate exhibiting a one-electron redox couple for metal in the surface layer can perform a 14-electron oxidation of butane to maleic anhydride. The possibility of an intermediate hopping or walking on the surface to various oxidized vanadium centers is unlikely due to the lack of observation of intermediately oxidized compounds, such as butadiene, in the butane pulse experiments. Such a migration process would weaken the interaction of the hydrocarbon with the catalyst and increase the probability of desorption, resulting in the formation of partially oxidized products. The observed unique dynamic nature of the surface layer of β-$(VO)_2P_2O_7$ with respect to oxygen and hydrogen exchange/migration on the reaction time scale suggests a different picture. The process could involve the shuttling of hydrogen away from and oxygen toward the intermediate adsorbed on the surface, with oxidation proceeding until the species (i.e., maleic anhydride) is able to desorb from the catalyst surface.

Acknowledgment. We thank Kim M. Shaw and Frank M. Bockhoff for performing the GC/mass spectrometry experiments, James D. Burrington for helpful discussions, and Edward M. Kostiner, University of Connecticut, for experimental assistance and consultation. The support of this work by SOHIO is acknowledged and greatly appreciated.

Registry No. $CH_3(CH_2)_2CH_3$, 106-97-8; β-$(VO)_2P_2O_7$, 58834-75-6; D_2, 7782-39-0.

(21) Adams, C. H. "Proceedings of the Third International Congress on Catalysis, Amsterdam 1964"; North Holland: Amsterdam, 1965; Vol. 1, p 240.

(22) Drago, R. S. *Coord. Chem. Rev.* **1980**, *32*, 111.

(23) Liu, H.-F.; Liu, R.-S.; Liew, K. Y.; Johnson, R. E.; Lunsford, J. H. *J. Am. Chem. Soc.* **1984**, *106*, 4117.